Fast assembly of the Coulomb matrix: A quantum chemical tree code

Matt Challacombe, Eric Schwegler, and Jan Almlöf

Citation: The Journal of Chemical Physics **104**, 4685 (1996); doi: 10.1063/1.471163
View online: http://dx.doi.org/10.1063/1.471163
View Table of Contents: http://scitation.aip.org/content/aip/journal/jcp/104/12?ver=pdfcov
Published by the AIP Publishing

Fast assembly of the Coulomb matrix: A quantum chemical tree code

Matt Challacombe, Eric Schwegler, and Jan Almlöf
Department of Chemistry, University of Minnesota, and Minnesota Supercomputer Institute, 1200 Washington Ave., South Minneapolis, Minnesota 55415

(Received 2 October 1995; accepted 13 December 1995)

Fast methods based on a representation of the electron charge density in a Hermite Gaussian basis are introduced for constructing the Coulomb matrix encountered in Hartree-Fock and density functional theories. Simplifications that arise from working in a Hermite Gaussian basis are discussed, translations of such functions are shown to yield rapidly convergent expansions valid in both the near- and far-field, and the corresponding truncation errors are derived in compact form. The relationship of such translations to hierarchical multipole methods is pointed out and a quantum chemical tree code related to the Barnes-Hut method is developed. Novel methods are introduced for the independent thresholding of ''bra'' and ''ket'' distributions as well as for screening out insignificant multipole interactions. Recurrence relations for computing the Cartesian multipole tensor are used to efficiently calculate far-field electrostatic interactions using high-order expansions. Application of the quantum chemical tree code to assembly of the Coulomb matrix for HF/3-21G calculations on sequences of polyglycine α-helices and water clusters demonstrate scalings as favorable as $N^{1.6}$, where N is the number of basis functions. Comparisons with a commercial electronic structure program indicate that our method is highly competitive. Speed is obtained without sacrificing precision, truncation errors are controlled with a single parameter, and the method performs equally well with a contracted or uncontracted LCAO basis. © *1996 American Institute of Physics.* [S0021-9606(96)01711-5]

I. INTRODUCTION

The solution of the Hartree-Fock equations by expanding their eigenfunctions in a set of atomic orbitals (LCAO)[1–5] leads to algorithms with a formal operation count proportional to N^4, where N is the number of LCAO basis functions. This N^4 dependence is associated with the evaluation and processing of the four-index electron repulsion integrals (ERIs)

$$(\phi_a\phi_b|\phi_c\phi_d)=\int d\mathbf{r}\int d\mathbf{r}'\,\phi_a(\mathbf{r})\phi_b(\mathbf{r}) \times|\mathbf{r}-\mathbf{r}'|^{-1}\phi_c(\mathbf{r}')\phi_d(\mathbf{r}'). \quad (1)$$

For molecular calculations, the LCAO basis functions of choice are the Cartesian Gaussian-type basis functions (CGTFs)

$$\phi_a(\mathbf{r})=(x-A_x)^{l_a}(y-A_y)^{m_a}(z-A_z)^{n_a} \times\exp[-\zeta_a(\mathbf{r}-\mathbf{A})^2], \quad (2)$$

introduced by Boys.[6] The four-index ERIs are required for evaluation of the Coulomb matrix **J** and the exchange matrix **K**, both of which are formed by contraction of four-index ERIs with the density matrix **D** as

$$J_{ab}=\sum_{cd} D_{cd}(\phi_a\phi_b|\phi_c\phi_d), \quad (3)$$

and

$$K_{ab}=\sum_{cd} D_{cd}(\phi_a\phi_c|\phi_b\phi_d). \quad (4)$$

It has been known since 1973[7,8] that in large systems a majority of the ERIs are insignificant, and that their thresholding leads to algorithms that are asymptotically of order $N^2\log N$ or even N^2,[8] depending on the thresholding criterion employed. However, thresholding integrals by size alone is not optimal,[8] and criteria based on significance to the total energy[9] may result in poor convergence or even divergence of the SCF procedure.[10,11] With direct SCF methods,[10–12] errors in elements of the Fock matrix $F_{ab}=J_{ab}-K_{ab}$ are controlled by thresholding density weighted ERIs, such as those occurring in Eqs. (3) and (4). The more sophisticated screening approaches made possible by direct methods are efficient, as even large ERIs may often be neglected if corresponding elements of the density matrix are small. They are also numerically stable as small ERIs will be retained if their contribution to the Fock matrix is predicted to be significant. Increases in computer power and the development of highly efficient recurrence relations for the computation of ERIs[13–24] have extended the applicability of direct technologies to molecules large enough that the N^2 limit has been approached very closely.[25]

It has been argued[26–28] that it is the calculation of ERIs significant to the Coulomb matrix that are responsible for this N^2 limitation, and that computation of the exchange matrix should scale as N for non-metallic systems due to the exponential decay of the exchange interaction.[26,29,30] This property has recently been exploited by Hernández *et al.*,[31] who use the exponential decay of the real space density matrix $\rho(\mathbf{r},\mathbf{r}')$ with $|\mathbf{r}-\mathbf{r}'|$ to obtain a linear scaling DFT technique. We will not belabor this issue further; instead we simply note that decoupling the computation of exchange and Coulomb matrices provides the freedom to pursue different specialized algorithms for the evaluation of each. This separation is required, or at least useful, in a number of advanced theoretical models such as DFT,[32,33] hybrid HF/DFT

methods[34,35] and the Møller–Plesset family of perturbation methods.[36–38] It may also facilitate computational developments, as for example parallel implementations on small-memory architectures.[39] Here, we restrict our presentation to the development of specialized mathematical and algorithmic methods for computation of the Coulomb matrix.

To discuss the $\mathcal{O}(N^2)$ limit of direct SCF methods, and the fast methods that may be used to overcome this limit, it is useful to first consider the Gaussian product theorem (GPT). The GPT states that an uncontracted distribution $\rho_{ab}=\phi_a\phi_b$ can be expressed exactly as a finite sum of CGTFs with exponent $\zeta_p=\zeta_a+\zeta_b$. For example, the product of two s-type Gaussians is

$$\exp[-\zeta_a(\mathbf{r}-\mathbf{A})^2]\times\exp[-\zeta_b(\mathbf{r}-\mathbf{B})^2]=$$
$$\exp[-\xi(\mathbf{A}-\mathbf{B})^2]\times\exp[-\zeta_p(\mathbf{r}-\mathbf{P})^2], \tag{5}$$

where $\xi=\zeta_a\zeta_b/\zeta_p$ and $\mathbf{P}=(\zeta_a\mathbf{A}+\zeta_b\mathbf{B})/\zeta_p$. As the system size increases, the radial overlap $\exp[-\xi(\mathbf{A}-\mathbf{B})^2]$ falls as a Gaussian with separation of the two centers A and B, and the number of distributions significant to the density, $\rho(\mathbf{r})=\Sigma_{ab}D_{ab}\rho_{ab}(\mathbf{r})$, approaches N from above. Likewise, the number of Coulomb matrix elements, $J_{ab}=(\rho_{ab}|\rho)$, larger than some small threshold is also $\mathcal{O}(N)$. Therefore, computation of the Coulomb matrix by conventional direct methods is at best an $\mathcal{O}(N^2)$ process.

Calculation of the Coulomb matrix is similar in many ways to the classical N-body problems encountered in molecular modeling and astrophysics. A variety of fast hierarchical methods that significantly reduce the complexity of such N-body problems have recently been introduced.[40–53] A common feature of these methods is that they subdivide space into a hierarchy of cubes (cells), and rely on a tree-like data structure, commonly called the Barnes–Hut (BH) tree. Starting with the root (parent), which contains all particles, space is recursively subdivided into smaller cells (children). The complexity of the computation can be reduced by approximating particle distributions within a cell as a series (multipole) expansion that converges rapidly in the far-field. Computations involving the hierarchy of cells are effective because the series expansions become increasingly more accurate with separation; larger cells may be used as the interaction distance increases.

Hierarchical methods may also be used to compute far-field components of the Coulomb matrix in quantum chemistry.[28,54] However, unlike the classical N-body problem, quantum chemical methods involve continuous distributions. Integrals that involve non-penetrating charge distributions may be efficiently evaluated with multipole methods. However, computing far-field components of the Coulomb matrix requires that integrals with overlapping charge distributions be set apart and computed by methods that are valid in the near-field. The problem is complicated by the fact that the near/far distinction depends on the extent (rate of decay) of the charge distributions as well as their separation. This should be contrasted with systems of point charges, wherein extents are vanishing and the term far-field refers only to the convergence of a multipole expansion.

This paper is organized as follows: In Sec. II we review both classical and quantum chemical hierarchical multipole methods. In Sec. III, we discuss the economies that may be realized by transforming the density into a basis of Hermite Gaussian-type functions (HGTFs). In Sec. IV, we examine the translation of HGTFs and show that they result in series expansions that are rapidly convergent both in the near- and far-field, and point out the relationship of these translations to hierarchical multipole methods. In Sec. VI, we introduce novel methods for the independent thresholding of "$\langle BRA|$" and "$|KET\rangle$" contributions to the Coulomb matrix as well as a new method for the distance dependent screening of insignificant far-field contributions. In Sec. VII, we discuss implementation of these methods in a quantum chemical tree code (QCTC). Then, in Sec. VII A we present timings obtained with QCTC and with GAUSSIAN 94 for HF/3-21G calculations on sequences of polyglycine α-helices and water clusters, demonstrating sub-N^2 scalings for assembly of the Coulomb matrix. In Sec. VII B we discuss these results and possible improvements of the method, and, finally, in Sec. VIII we draw conclusions from our results and findings.

II. HIERARCHICAL MULTIPOLE METHODS

Hierarchical multipole methods may be classified according to the type of multipole interactions computed. The two most common methods are the Barnes–Hut (BH)[40–46] and the fast multipole method (FMM).[47–51] Both the original BH and FMM methods employ a BH tree, the leaves of which are cells ideally containing a single particle. The BH method uses low-order Cartesian multipole approximations, while the FMM has traditionally relied on high-order spherical tensors.

The BH method computes particle-cell multipole interactions, and employs a multipole acceptability criteria (MAC)[45,46] to determine their validity; failure to meet the MAC results in recursion down the (inverted) tree to smaller cells, which may or may not meet the MAC. Ultimately, the algorithm reaches the lowest level (leaves) and computes all remaining interactions directly.

The FMM is characterized by interactions between cells wherein a far-field multipole expansion representing the potential of one cell is transformed into a locally convergent Taylor series expansion in another, which is well-separated from the first. Following these multipole-to-local (M2L) translations, the local Taylor expansions are passed down the tree accumulating the far-field potential from all well-separated cells. At the lowest level, interactions between a particle and all well-separated cells are evaluated with the Taylor series coefficients. Finally, remaining near-field interactions are evaluated directly.

Central to the FMM is the "well-separated" index (WSI), which for a given expansion order specifies the minimum number of intervening cells that guarantee convergence of all far-field expansions. Though rigorous, the FMM defi-

nition of what constitutes a pair of well-separated cells is based on a worst case error analysis of *all* the particles in a cell interacting with *all* the particles in another. On the other hand, the use of MACs in BH methods may lead to significantly tighter error estimates. While there are well known cases where MACs such as the BH opening criteria can lead to exploding galaxies and other (numerical) catastrophes,[45] rigorous MACs suitable for use with Cartesian multipoles have recently been developed.[46]

The most costly step in the FMM is the M2L ''horizontal'' translation that scales as $\mathcal{O}(\mathscr{L}^2)$ in two dimensions and as $\mathcal{O}(\mathscr{L}^4)$ in three dimensions,[43,49,50] where $\mathscr{L}$ is the order of the multipole expansion (the symbol p is often used instead of $\mathscr{L}$). To circumvent this $\mathscr{L}^4$ dependence, Elliot and Board have recently used the fast Fourier transform to reduce the cost of the M2L step to $\mathcal{O}(\mathscr{L}^2 \log \mathscr{L})$,[52] however, incurring a big increase in memory requirements and obtaining actual speedups of at most a factor of 2. Another approach is to simply reduce $\mathscr{L}$ [55,56] until the calculation is sufficiently fast, although the resulting errors may become excessively large in such a case. A third approach to circumventing the $\mathscr{L}^4$ bottleneck is to make the FMM more like the BH method. Such a hybrid FMM-BH method, dubbed the parallel multipole tree code (PMTA), has recently been introduced,[53] and involves use of the M2L translation between different sized cells and its more aggressive application when validated by a BH-like MAC. The PMTA is similar in many ways to the cell-cell interactions introduced by Warren and Salomon.[46]

Although the FMM has traditionally made use of high-order expansions in spherical harmonics, several Cartesian variants, called cell multipole methods (CMM), have also been developed.[56–59] Like the BH methods, the CMMs make use of low-order Cartesian multipole expansions. Also, CMMs do not employ rigorous error bounds, but rely on a WSI equivalent to the BH opening criteria.[56]

An important concept in the discussion of hierarchical methods is their computational complexity, i.e., the asymptotic dependence of cpu time on system size. The BH algorithm is usually cited as $\mathcal{O}(N \log N)$ and the FMM as $\mathcal{O}(N)$. It is generally accepted that for three dimensional systems the constants of proportionality associated with the BH $N\log N$ are much smaller than the associated constants of the FMM.[43,60,61] On the other hand, it is sometimes argued that the FMM may be faster for very large systems by virtue of its $\mathcal{O}(N)$ scaling.[48,51,62]

A key factor in the derivation of the aforementioned complexity estimates is the assumption of homogeneity,[62] under which all N particles are partitioned at a tree depth of $\log_8 N$. Recently, Aluru *et al.*[63] have argued that the complexity of both the BH and the FMM are distribution dependent; in the most favorable case they scale as $\mathcal{O}(N(\log N)^4)$ and at worst they are unbounded. These authors reason that the FMM and BH methods become unbounded when the BH tree involves long paths in which every cell contains the same set of particles. Such paths are the result of inhomogeneities, and may be arbitrarily large if the BH tree is extended to resolve all particles. On the other hand, if the BH tree is truncated before the particle distribution is well resolved, a substantial $\mathcal{O}(N^2)$ amount of work may be left to perform directly.

We disagree with the claim that the FMM necessarily involves a BH tree extending to the finest level of particle resolution and is therefore potentially unbounded. The FMM originally proposed by Greengard[62] involves recursion to a depth of $\log_8 N$, while most modern implementations of the FMM are adaptive,[64] and treat the BH tree depth as a tuning parameter.[51,56,64,65] Even if large trees with redundant nodes are generated, it is inexpensive to simply prune them before they are used. Furthermore, elegant particle decomposition methods which avoid redundancies are available.[66]

The utility of hierarchical methods for calculation of the Coulomb matrix has recently been discussed. The Q-Chem initiative has introduced the continuous fast multipole method (CFMM),[28] which is an adaptation of the Greengard FMM that accounts for the various distributions using a modified WSI. The CFMM WSI specifies the number of intervening cells that certify *both* the absence of penetration effects *and* convergence of the multipole expansion. For a given cell, the CFMM allows the summation of multipole moments only for distributions with identical WSIs. As moments are passed up the tree (to larger cells) the WSI is halved and the multipole moments of more distributions may be summed. The CFMM employs a truncated BH tree, obtained by subdividing the parent cell to obtain children in which the number of particles are approximately independent of the total number.[28,51] The CFMM employs conventional integral methods for direct computations and a 10^{-10} cutoff to eliminate insignificant distributions.

Kutteh, Aprá, and Nichols have recently discussed using generalized versions of the CMM (GCMM) or FMM (GFMM)[54] for Hartree-Fock and DFT calculations, and are currently implementing them in the electronic structure program NWChem. These methods are generalized in the following way: First, they are capable of handling point moments higher than monopole.[58,59] Secondly, three distinct contributions to the potential are considered at the finest level of spatial descretization: the near-field which is evaluated numerically by solving Poisson's equation; an intermediate region where straightforward multipole expansions are employed; and a Taylor-region which corresponds to the conventional FMM or CMM far-field. Also, unlike the CFMM, the GCMM or GFMM group all charge distributions within a cell and perform the succeeding upward and downward passes on the entire group; these authors claim that this makes the method intrinsically more efficient than CFMM. However, like the CFMM, the GCMM or GFMM also employ a truncated BH tree, which is determined by performance and accuracy issues.

The ''best'' hierarchical method for simulation of classical point charges is already a controversial topic, and the additional complexities introduced by continuous charge distributions are likely to make quantum chemical adaptations of such methods even more contentious. In the quantum case, applicability of the multipole approximation is limited not only by distance, but also by the extent (diffuseness) of

the charge distribution. Combining distributions with different extents makes computing the far-field component more efficient, but increases the cost of computing near-field interactions.

Very recently, the CFMM has been combined with the "very fast" FMM due to Petersen *et al.*,[49,50] yielding an algorithm referred to as "the Gaussian very fast multipole method" (GvFMM).[67] Like the CFMM, the GvFMM employs a measure of extent that is based on a worst case error analysis of *all* like-distributions (having the same exponent) in a cell interacting with *all* distributions in another. As a result, the GvFMM is dominated by calculation of the near-field integrals. The trade-offs between computation of near- and far-field are certainly dependent on the hierarchical method employed, on the method used for computation of near-field contributions, as well as on the specific implementation, computational platform, and level of precision required.

III. HERMITE GAUSSIAN-TYPE BASIS FUNCTIONS AND A SIMPLIFIED APPROACH TO CALCULATION OF THE COULOMB MATRIX

The McMurchie and Davidson (MD) algorithm[68–70] for the evaluation of CGTF-based ERIs was one of the first to employ recurrence relations. In the MD algorithm, the products of CGTFs describing elementary charge distributions are expanded exactly in HGTFs as

$$\rho_{ab}(\mathbf{r}) \equiv \phi_a(\mathbf{r})\,\phi_b(\mathbf{r}) = \sum_{L}^{l_a+l_b} \sum_{M}^{m_a+m_b} \sum_{N}^{n_a+n_b} e^{ab}_{LMN} \Lambda^{p}_{LMN}(\mathbf{r}), \tag{6}$$

where e^{ab}_{LMN} is an expansion coefficient obtained with the MD two-term recurrence relation and multiplied with the corresponding radial overlap. The HGTFs are defined by

$$\begin{aligned}\Lambda^{p}_{LMN}(\mathbf{r}) &= \frac{\partial^L}{\partial P_x^L}\frac{\partial^M}{\partial P_y^M}\frac{\partial^N}{\partial P_z^N}\exp[-\zeta_p(\mathbf{r}-\mathbf{P})^2] \\ &= \zeta_p^{(L+M+N)/2} H_L[\zeta_p^{1/2}(x-P_x)] \\ &\quad \times H_M[\zeta_p^{1/2}(y-P_y)] H_N[\zeta_p^{1/2}(z-P_z)] \\ &\quad \times \exp[-\zeta_p(\mathbf{r}-\mathbf{P})^2],\end{aligned} \tag{7}$$

where H_L is the L^{th} order Hermite polynomial. By analogy with Eq. (6), four-center CGTF-based ERIs may be transformed into linear combinations of the two-center HGTF-based ERIs

$$(\Lambda^{p}_{LMN}|\Lambda^{q}_{L'M'N'}) = \int d\mathbf{r} \int d\mathbf{r}'\, \Lambda^{p}_{LMN}(\mathbf{r})|\mathbf{r}-\mathbf{r}'|^{-1} \times \Lambda^{q}_{L'M'N'}(\mathbf{r}'). \tag{8}$$

The reduction of four-center ERIs to a short sum of two-center integrals is a direct consequence of the GPT. When CGTF distributions are expressed in a HGTF representation as in Eq. (6), the resulting two-center ERIs may be further reduced to a one-center form by noting that $\partial|\mathbf{P}-\mathbf{Q}|/\partial P_i = -\partial|\mathbf{P}-\mathbf{Q}|/\partial Q_i$ and re-writing them as

$$\begin{aligned}(\Lambda^{p}_{LMN}|\Lambda^{q}_{L'M'N'}) &= (-1)^{L'+M'+N'}(\Lambda^{p}_{L+L',M+M',N+N'}|\Lambda^{q}_{000}) \\ &= (-1)^{L'+M'+N'} u_{pq} R^{pq}_{L+L',M+M',N+N',0},\end{aligned} \tag{9}$$

where

$$R^{pq}_{lmn0} = \frac{\partial^l}{\partial PQ_x^l}\frac{\partial^m}{\partial PQ_y^m}\frac{\partial^n}{\partial PQ_z^n} F_0(\tau) \tag{10}$$

are "auxiliary functions,"

$$u_{pq} = \frac{2\pi^{5/2}}{\zeta_p\zeta_q\sqrt{\zeta_p+\zeta_q}}, \tag{11}$$

and PQ_x, PQ_y and PQ_z are the Cartesian components of $\mathbf{P}-\mathbf{Q}$. The auxiliary functions are related to the 0th order reduced incomplete gamma function,[71,72] which is

$$F_0(\tau) = \sqrt{\frac{\pi}{4\tau}}\,\mathrm{erf}(\sqrt{\tau}) = \int_0^1 e^{-\tau u^2} du, \tag{12}$$

with argument

$$\tau = \omega|\mathbf{P}-\mathbf{Q}|^2, \tag{13}$$

where

$$\omega = \frac{\zeta_p\zeta_q}{\zeta_p+\zeta_q}. \tag{14}$$

Differentiation of F_0 leads to higher order reduced incomplete gamma functions $F_{j+1} = -F_j'$, which we refer to hereafter simply as "gamma" functions.

For a class of HGTF-based ERIs with $L+M+N \leqslant \mathscr{L}_p$, $L'+M'+N' \leqslant \mathscr{L}_q$ and $\mathscr{L} = \mathscr{L}_p + \mathscr{L}_q$, the MD algorithm efficiently calculates all $\binom{\mathscr{L}+3}{3}$ auxiliary functions $R^{pq}_{l,m,n,0}$ with $l+m+n \leqslant \mathscr{L}$ from an initial set,

$$R^{pq}_{000j} = (-2\omega)^j F_j(\tau) \quad (j = 0,1,\ldots,\mathscr{L}), \tag{15}$$

using recursion relations[68–70] involving work that scales approximately as $\binom{\mathscr{L}+4}{4}$.

Since the total number of HGTF-based ERIs grows as $\binom{\mathscr{L}_p+3}{3}\times\binom{\mathscr{L}_q+3}{3}$, the cost per HGTF-based ERI decreases with increasing $\mathscr{L}_p$ and $\mathscr{L}_q$. In a conventional calculation, this economy is offset by the costly back-transformation to a Cartesian representation. The standard MD algorithm for evaluating the Coulomb matrix,

$$\begin{aligned}J_{ab} &= \sum_{cd} D_{cd}\, u_{pq} \sum_{L}^{l_a+l_b} \sum_{M}^{m_a+m_b} \sum_{N}^{n_a+n_b} e^{ab}_{LMN} \\ &\quad \times \sum_{L'}^{l_c+l_d} \sum_{M'}^{m_c+m_d} \sum_{N'}^{n_c+n_d} (-1)^{L'+M'+N'} e^{cd}_{L'M'N'} \\ &\quad \times R^{pq}_{L+L',M+M',N+N'},\end{aligned} \tag{16}$$

involves four-fold loops over basis functions a,b,c and d, inside of which the expensive HGTF to CGTF transformation over LMN and $L'M'N'$ takes place. However, if the density matrix is first transformed to an HGTF basis as

$$E^q_{L'M'N'} = \sum_{cd} D_{cd} e^{cd}_{L'M'N'}, \tag{17}$$

significant economies may be realized. This is the approach introduced by Ahmadi and Almlöf,[73] and shares certain features with the "*J* Matrix Engine" of White and Head-Gordon.[74]

Asymptotically, transformation of the density into an HGTF representation requires effort and memory proportional to N and avoids the costly transformation from HGTF to CGTF inside the four-fold loop over basis functions. Representation of the density in an HGTF basis also allows dramatic simplifications when the LCAO basis set shares exponents between CGTFs of different angular symmetry. Examples of such "family" basis sets include the Pople sp-type functions,[75] the well-tempered basis sets of Huzinaga and co-workers,[76–79] the even-tempered basis sets of Bardo and Ruedenberg,[80] the geometrical basis sets of Clementi and Corongiu,[81] and Wilson's universal basis set.[82,83]

The expansion of CGTF distributions leads to HGTF families that are all related to a "mother" (s-type) Gaussian by differentiation. Using family LCAO basis sets is economical because *all* CGTF distributions in a LCAO family are then related to the corresponding family of HGTFs by Eq. (6). The benefits obtained with a family LCAO basis set are two-fold. First of all, the redundancies associated with equivalent combinations of CGTF angular symmetries may be eliminated. For example, p-p and s-d products that share the same exponent and center correspond to the same family of HGTFs and their contributions to the density may be summed. Secondly, as the MD algorithm computes all R_{lmn} with $l+m+n \leqslant \mathscr{L}$, auxiliary functions with $l+m+n < \mathscr{L}$ are obtained at no additional cost.

Our algorithm for computing the Coulomb matrix in a HGTF basis involves the accumulation of contributions to the HGTF family p from all HGTF families q that constitute the density;

$$\mathscr{J}_{p,LMN} = \sum_q u_{pq} \sum_{L'M'N'} (-1)^{L'+M'+N'} \times E^q_{L'M'N'} R^{pq}_{L+L',M+M',N+N'}. \tag{18}$$

All elements of the Coulomb matrix belonging to CGTF distributions in family p may then be evaluated as

$$J_{ab} = \mathbf{e}^{ab} \cdot \mathscr{J}_p, \quad J_{a'b'} = \mathbf{e}^{a'b'} \cdot \mathscr{J}_p, \quad \ldots \ (ab, a'b', \ldots \in p), \tag{19}$$

where elements of the vectors $\mathbf{e}^{ab}$ and $\mathscr{J}_p$ have been conveniently arrayed using the canonical index

$$LMN = \binom{L+M+N+2}{3} + \binom{M+N+1}{2} + N + 1. \tag{20}$$

The benefits of using a family LCAO basis should now be obvious: As the work associated with Eq. (17) and Eq. (19) takes place outside the four-fold loop over basis functions, the limiting step is the evaluation of the auxiliary functions R^{pq}_{lmn} and their contraction as in Eq. (18), both of which are proportional to the square of the number of HGTF families. If family LCAO basis sets are employed, the total number of HGTF families can be reduced dramatically.

IV. FAST HERMITE GAUSSIAN METHODS

Hermite Gaussian functions may be expressed in terms of other HGTFs at other centers using rapidly convergent series expansions. In the far-field, such translations are equivalent to the manipulations used in hierarchical multipole methods. However, unlike multipole expansions, these translations result in series that are convergent in the near-field and form the basis of the fast Gauss transform. In the following, properties of these expansions are examined, the near/far-field distinction is discussed, and the applicability of such translations under various conditions are considered.

A. The fast Gauss transform and the translation of HGTFs

The fast Gauss transform (FGT)[84–86] was originally developed to accelerate the numerical solution of the heat equation involving a Gaussian kernel. Like the BH and FMM, the FGT is a clustering technology that relies on rapidly convergent series to reduce complexity. Although originally employed as a device to accelerate quadrature, the adaptation presented here preserves the integrity associated with the analytic evaluation of two-electron integrals.

Starting with the generating function of the Hermite polynomials,

$$\exp(2xt - t^2) = \sum_{k=0}^{\infty} \frac{t^k}{k!} H_k(x), \tag{21}$$

it is elementary to show

$$\exp[-\zeta(r-q)^2] = \exp[-\zeta(r-c)^2] \sum_{k=0}^{\infty} \frac{(q-c)^k}{k!} \times \zeta^{k/2} H_k[\zeta^{1/2}(r-c)], \tag{22}$$

which is the translation of a one-dimensional s-type HGTF from center c to center q expressed as a series that is *both* a Taylor and a Hermite expansion. The key feature of Eq. (22) is that this series converges rapidly both locally and in the far-field. In the near-field, the convergence of expansions involving large translations and diffuse distributions is noteworthy. In Fig. 1, we illustrate this convergence with an unnormalized one-dimensional s-type Gaussian having exponent $\zeta = 0.1$ and its translation 2.5 au with a finite expansion of order $\beta = 5$. Likewise, in three dimensions arbitrary HGTFs may be translated as

$$\Lambda^q_{LMN}(\mathbf{r}) = \sum_{UVW}{}' \left[(Q_x - C_x)^U (Q_y - C_y)^V (Q_z - C_z)^W \times \frac{\Lambda^c_{(L+U,M+V,N+W)}(\mathbf{r})}{U!V!W!} \right] + \epsilon^{q\to c}_{(LMN,\beta)}(\mathbf{r}), \tag{23}$$

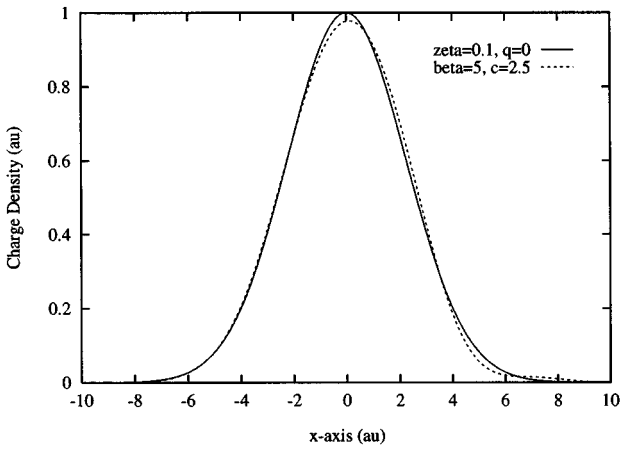

FIG. 1. An unnormalized one-dimensional s-type Gaussian with $\zeta=0.1$ centered at $q=0$ and its expansion about $c=2.5$ with $\beta=5$.

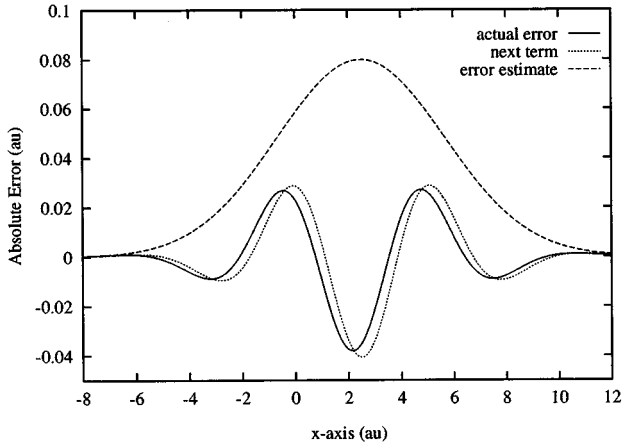

FIG. 2. The actual error, the error estimate given by Eq. (27) and the next $(\beta+1=6)$ term corresponding to the expansion depicted in Fig. 1.

where the prime indicates the restricted summation $U+V+W\leqslant\beta$, $\epsilon^{q\to c}_{(LMN,\beta)}$ is the truncation error, and β is the order of the expansion.

Using Cramer's inequality[87]

$$H_\beta(x)\leqslant K2^{\beta/2}\sqrt{\beta!}e^{x^2/2}\quad(K<1.09) \tag{24}$$

and Stirling's approximation,

$$\beta!\approx\sqrt{2\pi\beta}(\beta/e)^\beta, \tag{25}$$

we obtain

$$\epsilon^{q\to c}_{(0,\beta)}(\mathbf{r})\leqslant\frac{K^3}{[2\pi(\beta+1)/3]^{3/4}}\left(\frac{6e\zeta_q\Delta^2}{\beta+1}\right)^{\frac{\beta+1}{2}}\times\exp\left(-\frac{\zeta_q}{2}|\mathbf{r}-\mathbf{C}|^2\right), \tag{26}$$

which is the error resulting from translation of a s-type Gaussian a distance less than Δ using an expansion truncated at order $U+V+W=\beta$. Equivalent error estimates may be obtained for higher-ℓ HGTFs, and show that they are more difficult to translate. The quality of $\epsilon^{q\to c}_{(0,\beta)}$ can be gauged by Fig. 2, where we show the error of the one-dimensional expansion in Fig. 1, the next term in that expansion, and the error estimate

$$\epsilon^{q\to c}_{(0,\beta)}(x)\leqslant\frac{K}{[2\pi(\beta+1)]^{1/4}}\left(\frac{2e\zeta_q\Delta^2}{\beta+1}\right)^{\frac{\beta+1}{2}}\times\exp\left[-\frac{\zeta_q}{2}(x-c)^2\right], \tag{27}$$

which is the one-dimensional analog of Eq. (26).

The McMurchie-Davidson algorithm evaluates all integrals $(\Lambda^p_{LMN}|\Lambda^q_{L'M'N'})$ with $L+M+N\leqslant\mathscr{L}_p$ and $\ell_q=L'+M'+N'\leqslant\mathscr{L}_q$ in $\binom{\mathscr{L}_p+\mathscr{L}_q+4}{4}$ cpu time. If, for a given expansion length β and corresponding cell width 2Δ, M_{cell} HGTFs of ℓ_q-type occupy a cell and

$$\binom{\mathscr{L}_p+\beta+4}{4}\ll\binom{\mathscr{L}_p+\mathscr{L}_q+4}{4}\times M_{\text{cell}}, \tag{28}$$

then a significant reduction in cpu time may be realized by employing the rapidly convergent expansion given by Eq. (23).

The efficiency of the FGT can be increased dramatically with secondary expansions about new exponents, further clustering distributions with closely related exponents. One such approach is to Taylor expand distributions with similar extents about a nearby exponent α. For an s-type function, such an approximation leads to the series

$$\exp[-\zeta_q(\mathbf{r}-\mathbf{Q})^2]=\sum_{l=0}^{n}\frac{(-\delta)^l}{l!}(\mathbf{r}-\mathbf{Q})^{2l}\times\exp[-\alpha(\mathbf{r}-\mathbf{Q})^2], \tag{29}$$

which is rapidly convergent if $\delta=\zeta_q-\alpha$ is small. We envision application of the FGT primarily for diffuse exponents that enter the far-field regime slowly (see the following Section). This will allow the use of large cells, viz. Eq. (26), and will permit the effective use of secondary expansions by virtue of the small exponents involved.

B. The far-field limit of HGTF-based ERIs and their translations

Hermite Gaussian functions are related to derivatives of the Dirac delta function by

$$\delta^{\,p}_{LMN}(\mathbf{r})=\frac{\partial^L}{\partial P_x^L}\frac{\partial^M}{\partial P_y^M}\frac{\partial^{\,N}}{\partial P_z^N}\delta(\mathbf{r}-\mathbf{P})=\lim_{\zeta_p\to\infty}\left(\frac{\zeta_p}{\pi}\right)^{3/2}\Lambda^p_{LMN}(\mathbf{r}). \tag{30}$$

The derivatives δ^p_{LMN} obey the identity[88]

$$\int d\mathbf{r}f(\mathbf{r})\delta^p_{LMN}(\mathbf{r})=(-1)^{L+M+N}\frac{\partial^L}{\partial P_x^L}\frac{\partial^{\,M}}{\partial P_y^M}\frac{\partial^{\,N}}{\partial P_z^N}f(\mathbf{P}). \tag{31}$$

When two HGTFs are close enough to interact significantly, yet far enough apart that charge penetration (overlap) between the two is negligible, Eqs. (30) and (31) may be used[89] to obtain

$$(\Lambda^p_{LMN}|\Lambda^c_{L'M'N'}) \approx (-1)^{L+M+N}\left(\frac{\pi}{\zeta_p}\right)^{3/2} T^{CP}_{L+L',M+M',N+N'}\left(\frac{\pi}{\zeta_c}\right)^{3/2}, \quad (32)$$

where T is the Cartesian multipole tensor (T-tensor) with rank ℓ elements

$$T^{CP}_{lmn}=\frac{\partial^{\ell}}{\partial CP_x^l \partial CP_y^m \partial CP_z^n}\frac{1}{|\mathbf{C}-\mathbf{P}|} \quad (\ell=l+m+n). \quad (33)$$

Equation (32) provides a seamless transition between the expansions employed in the fast Gauss transform and the Cartesian multipole expansion of $|\mathbf{r}-\mathbf{r}'|^{-1}$. The accuracy of this approximation increases with the distance $|\mathbf{C}-\mathbf{P}|$ between HGTFs because high ranking elements of the T-tensor decay rapidly with separation. For a given level of accuracy, this allows reduction of the expansion order β and/or the use of longer translations Δ with increasing separation. When penetration is negligible, the distinction between HGTFs and their multipole approximation might not seem important as reduction of the expansion order may be carried out with equal facility in either case. However, the multipole approximation permits the combination of moments sharing the same center, even if derived from distributions with different exponents. Thus, translations as in Eq. (23) may be used in combination with the multipole limit of HGTF-based ERIs, Eq. (32), to represent large numbers of distributions in a form with significantly reduced complexity.

It is also possible[89] to arrive at Eq. (32) directly using the asymptotic expression

$$F_j(\tau)=\frac{\pi^{1/2}(2j-1)!!}{2^{(j+1)}\tau^{(j+1/2)}}-\frac{e^{-\tau}}{2\tau} \quad (\tau\to\infty), \quad (34)$$

where $\tau=\omega|\mathbf{C}-\mathbf{P}|$ as in Eq. (13). Thus, applicability of the far-field limit to HGTF-based ERIs depends on both the separation of centers and the relative fall-off of the distributions, i.e., their non-penetration regardless of the distance separating them. The approximate behavior of errors introduced into translated ERIs by truncation of the expansion and by ignoring penetration effects may be obtained by considering $R^{cp}_{\ell}\equiv\partial^{\ell}F_0(\tau)/\partial|\mathbf{C}-\mathbf{P}|^{\ell}$ and Eq. (34) with $j=0$, from which we find

$$u^{cp}R^{cp}_{\ell}=\frac{\pi^3}{(\zeta_p\zeta_c)^{3/2}}\frac{\ell!}{|\mathbf{C}-\mathbf{P}|^{\ell+1}}-\frac{4\pi^{5/2}}{(\zeta_p+\zeta_c)^{3/2}} \times(2\omega|\mathbf{C}-\mathbf{P}|)^{\ell-2}e^{-\tau} \quad (\tau\to\infty). \quad (35)$$

As $R_{LMN}\leqslant R_{\ell}\forall\ell=L+M+N$, Eq. (35) is a gauge of convergence with respect to both expansion length and penetration. However, Eq. (35) pertains to convergence of the FGT in the multipole limit; when the near-field is computed directly, the second term in Eq. (35) should be replaced with an equivalent, expansion independent expression involving the order of the original distribution(s) angular symmetry. In either case, when the second term in Eq. (35) is sufficiently small, the electrostatic interaction between the HGTF family p and the HGTF family c is said to be of the "far-field" type. When ℓ corresponds to a given rank in a truncated series of ERIs (resulting from translation as in Eq. (23)), and the first term in Eq. (35) is negligible, the truncated multipole expansion is said to be acceptable.

Unfortunately, the penetration term in Eq. (35) is only useful in the accurate *a priori* estimation of errors for very large τ. However, one may always empirically determine a suitable value τ_{sw} which allows the unconditional use of the multipole approximation whenever $\tau>\tau_{\mathrm{sw}}$. This is the approach used in this work, as explained in Secs. VI and VII.

V. THE HIERARCHY OF MULTIPOLES

In the quantum chemical tree code (QCTC), distributions of all extents are combined in each cell c as it greatly simplifies computation of both near- and far-field contributions. The hierarchy of moments in QCTC forms an inverted oct-tree, which is a tree having 2^3 possible subcells belonging to each node. The smallest cells are at "ground level" in *tier* zero, referenced as $t=0$. This approach is a bottom up method similar to the Press tree,[90] and is contrary to conventional hierarchical methods that start with a single cell encompassing the entire system and recur down to smaller cells by subdivision. The advantage of our approach is that the smallest cell size influences both the efficiency of near-field computations and the applicability of the multipole approximation; by tuning Δ the two may be balanced.

Our oct-tree is formed as follows: First, all distributions within each cell c of half width Δ are translated to a point $\mathbf{C}$ at the center of the cell, and the moments of each cell in tier zero are computed. Next, these cells $c\equiv c^0$ are fused to form the next tier of cells that are twice as wide and eight times less numerous than those in the previous tier. In general, each cell c^t in tier t has half width equal to $\Delta_t=2^t\Delta$ and is centered at

$$\mathbf{C}^t=\mathbf{R}_{\mathrm{left}}+(2\mathbf{c}^t+1)\Delta_t, \quad (36)$$

where $\mathbf{R}_{\mathrm{left}}$ is the leftmost atom center and $\mathbf{c}^t$ is a list of indices particular to $\mathbf{C}^t$. With this scheme, the entire density is partitioned into the hierarchy of multipole moments

$$\varrho^{c^t}_{(U+L,W+M,V+N)}=\sum_{q\in c^t}(Q_x-C^t_x)^U(Q_y-C^t_y)^V \times(Q_z-C^t_z)^W\frac{E^q_{LMN}}{U!V!W!}\left(\frac{\pi}{\zeta_q}\right)^{3/2}, \quad (37)$$

where E^q_{LMN} was defined in Eq. (17) and

$$q\in c^t \text{ iff } c^t_i=\mathrm{int}\left(\frac{Q_i-R_{i,\mathrm{left}}}{\Delta_{t+1}}\right) \quad \forall i=x,y, \text{ and } z. \quad (38)$$

With the hierarchy of moments, the far-field potential at $\mathbf{P}$ may be computed as

$$\mathscr{J}^{\rm far}_{P,LMN}=\sum_{c^t}{}' \sum_{L'M'N'} T^{C^tP}_{L+L',M+M',N+N'}\varrho^{c^t}_{L'M'N'}, \quad (39)$$

where the prime indicates that the largest cells (and the lowest rank tensors) possible are always used (see Sec. VI), and that redundant calculations involving parent cells and their children are avoided. The far-field contribution to elements of the Coulomb matrix with distributions centered at P may then be computed as

$$J^{\rm far}_{ab}=\varrho^{ab}\cdot\mathscr{J}^{\rm far}_P \quad J^{\rm far}_{a'b'}=\varrho^{a'b'}\cdot\mathscr{J}^{\rm far}_P,$$
$$\ldots\ (ab,a'b',\ldots\in P), \quad (40)$$

where

$$\varrho^{ab}_{LMN}=(-1)^{L+M+N}\left(\frac{\pi}{\zeta_p}\right)^{3/2}e^{ab}_{LMN}. \quad (41)$$

VI. THRESHOLDING OF ⟨BRA|S AND |KET⟩S.

Conventional direct methods control truncation errors in elements of the Fock matrix by testing the (estimated) product between two-electron integrals and corresponding elements of the density matrix. However, in order to assign elements of the density to cells one must know *a priori* which distributions are significant. Also, thresholding at the level of integrals introduces additional work that may eventually dominate the entire calculation. It is therefore critical to independently gauge the significance of a $|KET\rangle$ distribution before its transformation into a HGTF representation, as well as the significance of a $\langle BRA|$ distribution prior to entering the four-fold loop over basis functions.

Our objective is to limit the error in $J_{ab}=(\rho_{ab}|\rho)$ to within

$$(\epsilon_1|\rho)+(\rho_{ab}|\epsilon_2)\sim\mathscr{O}(\text{thresh}), \quad (42)$$

where ϵ_1 and ϵ_2 represent neglected $\langle BRA|$ and $|KET\rangle$ distributions respectively, and where thresh is a thresholding parameter.

The neglect of a $\langle BRA|$ distribution introduces the error ϵ_1, which from Holder's inequality[91,92] obeys the bound

$$(\epsilon_1|\rho)\leqslant N_{\rm el}\int d\mathbf{r}|\mathbf{r}|^{-1}\epsilon_1(\mathbf{r}). \quad (43)$$

Assuming that the neglect of any $\langle BRA|$ distribution leads to an error that is on the same order of magnitude as that incurred by the neglect of an s-type distribution with the same exponent and center, we arrive at the thresholding criteria

$$\frac{2\pi}{\zeta_p}\exp\left[-\frac{\zeta_a\zeta_b}{\zeta_a+\zeta_b}(\mathbf{A}-\mathbf{B})^2\right]\leqslant\frac{\text{thresh}}{N_{\rm el}} \quad (44)$$

for neglect of *family* $\langle BRA|$ distributions involving exponent ζ_p and center P.

In an incremental Fock build, $N_{\rm el}$ in Eq. (44) can be replaced with

$$N'_{\rm el}=\sum_{ab}\Delta D_{ab}S_{ab}, \quad (45)$$

where $\Delta\mathbf{D}$ is the difference density matrix and S_{ab} is an element of the overlap matrix. As $\|\Delta\mathbf{D}\|$ becomes smaller, so too does $N'_{\rm el}$, and the criterion Eq. (44) may be relaxed accordingly.

To find a thresholding criteria for eliminating contributions to the density, we assume that $\epsilon_2\approx ND_{cd}\rho_{cd}$ is an average error that accrues from the neglect of $\mathscr{O}(N)$ marginally significant s-type distributions ρ_{cd}. Using the familiar Schwartz inequality,[12,93,94]

$$|(\rho_{ab}|\epsilon_2)|\leqslant(\epsilon_2|\epsilon_2)^{1/2}(\rho_{ab}|\rho_{ab})^{1/2}, \quad (46)$$

we arrive at the criterion

$$\zeta_q^{-5/4}\exp\left[-\frac{\zeta_c\zeta_d}{\zeta_c+\zeta_d}(\mathbf{C}-\mathbf{D})^2\right]\max(|D_{cd}|)\leqslant\left(\frac{\sqrt{2}\zeta_{\rm min}^{5/4}}{\pi^{5/2}N}\right)\text{thresh}, \quad (47)$$

for neglect of the HGTF family q, where the max is $\forall cd\in q$ and where we have taken $(\rho_{ab}|\rho_{ab})^{1/2}\approx 2^{1/4}(\pi/\zeta_{\rm min})^{5/4}$ with $\zeta_{\rm min}$ the smallest distribution exponent. Here too, we may replace $\max(|D_{cd}|)$ with $\max(|\Delta D_{cd}|)$ in an incremental Fock build.

Throughout our discussion we have assumed the use of an uncontracted basis set, partly for convenience and partly because the methods that we are developing do not benefit from contraction. However, if contraction is employed, the number of LCAO primitives should replace N and the max contraction coefficients should multiply the corresponding max density matrix elements in Eq. (47), as well as the LHS numerator of Eq. (44). Although the independent thresholding criteria, Eqs. (44) and (47), are not rigorous, they are correct to within an order of magnitude and take into account the size of the density matrix, the distribution exponent, and the radial overlap. They also incorporate the system size in the case of Eq. (44), and the basis set size in the case of Eq. (47). This approach offers substantial benefits, both in accuracy and efficiency, over the hard cutoff of 10^{-10} used in the CFMM.[28] Our approach to thresholding distributions is an inexpensive N^2 process which rapidly reduces the density and the Coulomb matrix to objects with $\mathscr{O}(N)$ complexity. Distributions with small exponents will enter the $\mathscr{O}(N)$ regime more slowly than those with large exponents. This is because our estimates depend on an inverse power of the exponent as well as on the radial overlap. A standard practice in many electronic structure programs is to threshold ERIs at the level of contracted shell-quartets[12] or shell-pairs.[24] However, many contraction schemes, e.g., 6-31G, couple exponents spanning 3 orders of magnitude. Thus the evaluation of a contracted shell-quartet is linked to the decay of the most diffuse distribution(s). In this context, rigorous inequalities[12,91] are clearly superior to non-rigorous estimates such as the contracted products of radial overlaps.[11] Nevertheless, no matter how tight the bound, *thresholding at the level of contracted functions inevitably leads to significant amounts of unnecessary work.*

Additionally, operating with an uncontracted basis, or at the level of primitives, is required by the Barnes-Hut (BH)

hierarchical multipole method discussed in Sec. II. This is because the center of each $\langle BRA|$ distribution must be considered individually. As mentioned above, one of the main advantages of the BH method is the aggressive use of multipole approximations, the validity of which are determined by multipole admissibility criteria (MACs). Commonly, MACs are used to determine the applicability of multipole expansions through some fixed order (typically monopole or quadrupole) for a given cell-particle separation. Here we introduce a dynamic MAC based on the bound

$$|T_{lmn}^{C^tP}| \leqslant \ell! |\mathbf{C}^t - \mathbf{P}|^{-(\ell+1)} \quad (\ell = l+m+n), \tag{48}$$

which leads to the criterion

$$\varrho^p_{\ell_o} \varrho^{c^t}_{\ell_{c^t}} (\ell_p + \ell_{c^t})! |\mathbf{C}^t - \mathbf{P}|^{-(\ell_p + \ell_{c^t}+1)} \leqslant \frac{\text{thresh}}{N_{c^t}}, \tag{49}$$

where N_{c^t} is the number of occupied cells in tier t, and $\varrho^{c^t}_{\ell_{c^t}}$ $\varrho^p_{\ell_p}$ are strengths of the corresponding moments that are determined as the backwards sum of the maximum multipole moments in each rank, where for example

$$\varrho^{c^t}_{\ell_{c^t}} = \sum_{\ell_{c^t} \leqslant j} \max_{j=L+M+N} (|\varrho^{c^t}_{LMN}|). \tag{50}$$

Because the multipole strengths decrease monotonically with rank, Eq. (49) may be used to determine not only admissibility of the multipole approximation but to radically prune the rank of both $\langle BRA|$ and $|KET\rangle$ moments for expansions that have met the MAC.

VII. A QUANTUM CHEMICAL TREE CODE

Although our code QCTC is still in rapid development, it is relevant to discuss its present implementation and to present results showing its promise. Our current implementation has been developed on the Cray C-90 and interfaced with the *ab initio* electronic structure program SUPERMOLECULE v1.1.[95] SUPERMOLECULE computes the conventional exchange and core Hamiltonian matrices, and calls QCTC to calculate the Coulomb matrix in each cycle of the iterative SCF process. In the spirit of the direct approach, QCTC does not store integrals, and recomputes all intermediates in every cycle. As explained in Sec. VI, the precision obtained with QCTC is controlled by a single thresholding parameter.

QCTC first transforms the density into a basis of significant HGTF family distributions and assigns them to cells in the zeroth tier. The significance of a family $|KET\rangle$ distribution is assessed with criterion Eq. (47) and the CGTF–HGTF transformation is carried out as in Eq. (6). Distributions are assigned to a particular cell with Eq. (38). Next, multipole moments are formed for the hierarchy of cells, and their genealogy is determined. A loop over significant $\langle BRA|$ HGTF families is then entered and validity of the multipole approximation is determined for far-field interactions between $\langle BRA|$ and $|KET\rangle$ moments of rank ℓ_p and ℓ_{c^t} respectively, starting with all cells in the highest tier (largest cells) and progressing to all cells in tier zero. The significance of a family $\langle BRA|$ distribution is assessed with Eq. (44) and the applicability of the far-field approximation is determined by the criteria $\tau_{\min} > \tau_{\text{sw}}$ and Eq. (49), where $\tau_{\min} = \zeta_p \zeta_{\min}/\zeta_p + \zeta_{\min}(\mathbf{C}-\mathbf{P})^2$ and $\zeta_{\min}$ is the smallest distribution exponent contributing to the cell moment under scrutiny. Expansions that meet the MAC, e.g., satisfy Eq. (49), are pruned on both sides by reducing ℓ_p to ℓ_{BRA} and ℓ_{c^t} to ℓ_{KET} such that Eq. (49) remains satisfied for $\ell_p = 0$ and $\ell_{c^t} = \ell_{\text{KET}}$ as well as for $\ell_p = \ell_{\text{BRA}}$ and $\ell_{c^t} = 0$. In this way, the work associated with computing the T-tensor is reduced from $\binom{\ell_p + \ell_{c^t} + 4}{4}$ to $\binom{\ell_{\text{BRA}} + \ell_{\text{KET}} + 4}{4}$. The T-tensor, Eq. (33), is calculated efficiently using recurrence relations.[89,96]

After the far-field interactions with a $\langle BRA|$ family have been computed, the remaining near-field interactions are calculated with Eq. (19) by looping over the remaining cells and loading buffers for evaluation of the auxiliary functions R_{lmn}. This buffering is accomplished with cell-based pointers, a process that becomes more efficient on vector computers as the cell size, and the corresponding lists, become larger. However, it will often be the case that many cells in the zeroth tier have contributed to the far-field, which means that the efficiency of addressing the density (on vector computers) is controlled by the size of cells in tier zero. On vector computers there is a definite trade-off between the calculation of near- and far-field contributions that is controlled by size of the smallest cell, as well as by the maximum order of the multipole expansion β and thresh. As QCTC is still in rapid development, we have not attempted to optimize these parameters for large systems. Instead, we have determined optimal parameters for a cluster of 10 water molecules at the HF/3-21G level of theory using thresh$=10^{-5}$. The current implementation of QCTC has the lowest execution times for this system with $\Delta = 1.65$ au, $\beta = 5$ and $t = 0, \ldots, 3$. With these parameters, we have found that choosing $\tau_{\text{sw}} = 13$ yields errors that are less than those introduced by thresholding.

A. Results

We have performed HF/3-21G calculations with SUPERMOLECULE/QCTC and GAUSSIAN 94[97] on the sequence of water clusters shown in Fig. 3 and the sequence of polyglycine α-helices shown in Fig. 4. (Input files for the sequence of structures featured in Figs 3 and 4 are available in both GAUSSIAN 94 and SUPERMOLECULE formats from the first author via e-mail to mf10111@msi.umn.edu). Although not shown in Figs. 3 and 4, these sequences include water clusters with 80 and 160 waters and helices with 24 and 48 residues, respectively. In Fig. 5, GAUSSIAN 94 and QCTC cpu times per SCF cycle are shown for the sequence of water clusters. Figure 6 shows comparable cpu times for the sequence of polyglycine α-helices. Included in Figs. 5 and 6 are matrix diagonalization timings for $N \times N$ symmetric matrices obtained with subroutine F02ABE of the NAG library.[98]

The timings shown in Figs. 5 and 6 are average cpu times for building the Coulomb matrix with QCTC and the average cpu time spent computing the Fock matrix and solving the SCF equations in GAUSSIAN 94. The latter operations represent approximately twice the work performed by QCTC, as LINK502 also computes the exchange matrix. Based on the

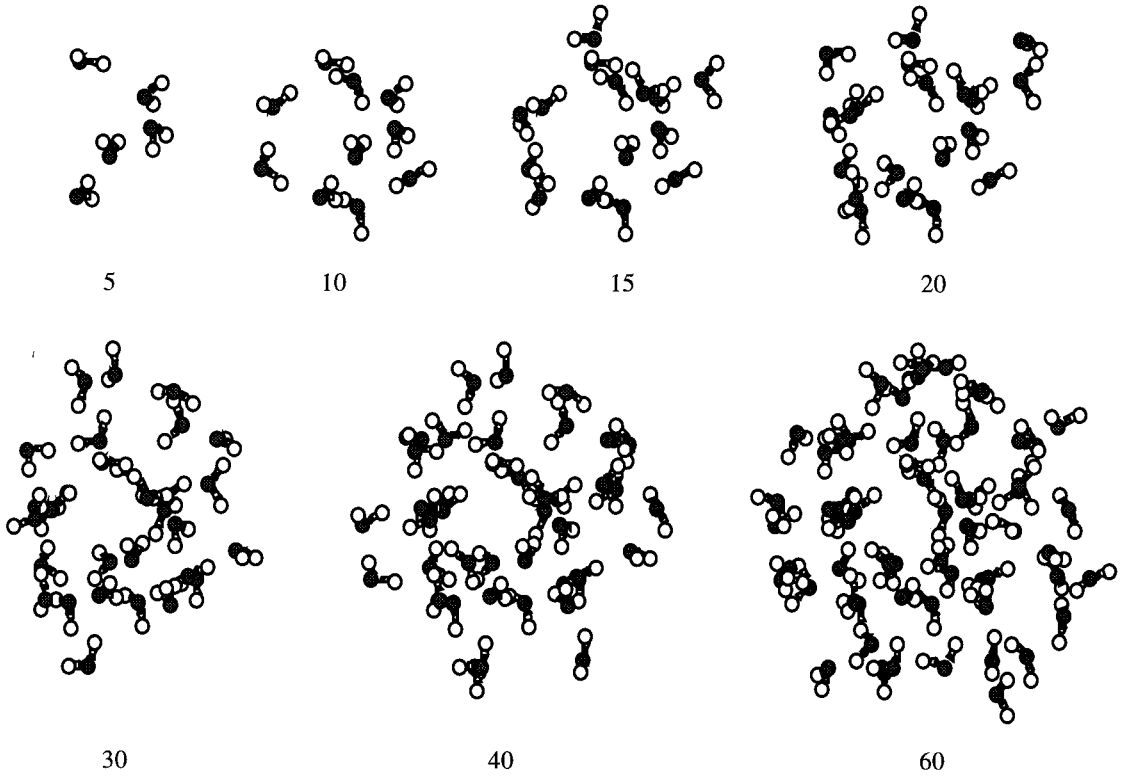

FIG. 3. A sequence of water clusters taken from an equilibrated molecular dynamics simulation corresponding to 25 °C and 1 atm. All water molecules have the fixed geometry $\angle_{HOH}=104.52°$ and $R_{OH}=0.957$Å.

diagonalization timings, LINK502 must be dominated by integral evaluation for the range of GAUSSIAN 94 timings reported in Figs. 5 and 6. All reported times were obtained with a single Cray C-90 processor[2] and all GAUSSIAN 94 timings refer to time spent in LINK502 using the SCF=(Direct,NoIncFock) options. (Cray cf77 compiler version 6.0.4.0 was used to compile QCTC with the following options: cf77 -c -Zc -Wf"-dp -m3 -i64 -es -a stack -o

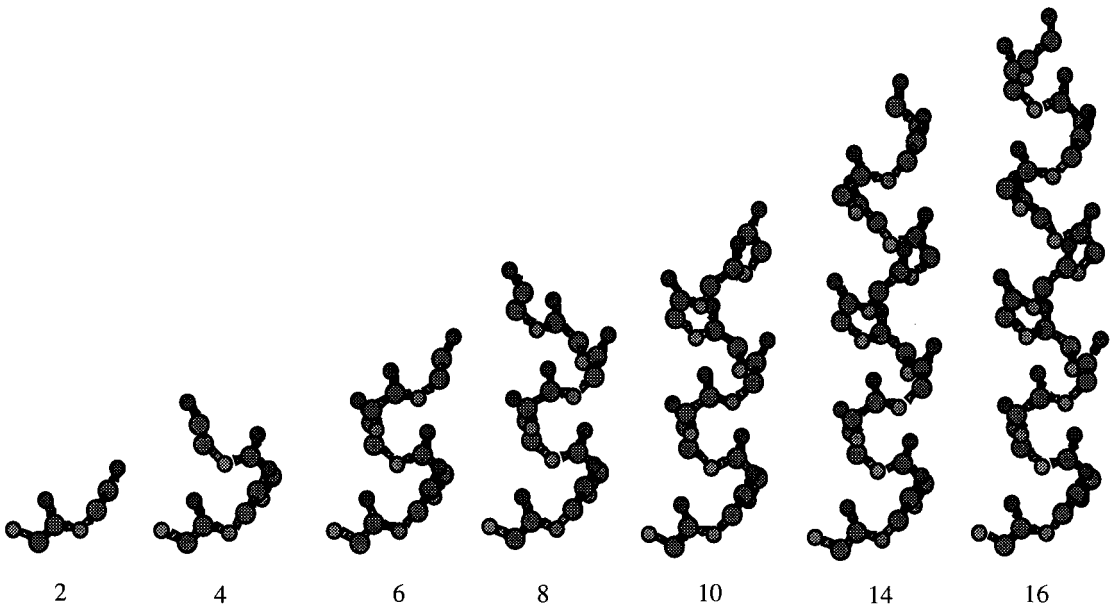

FIG. 4. A sequence of polyglycine α-helices. Coordinates were obtained with the Insight II program.[108] Some hydrogen atoms have been deleted for clarity.

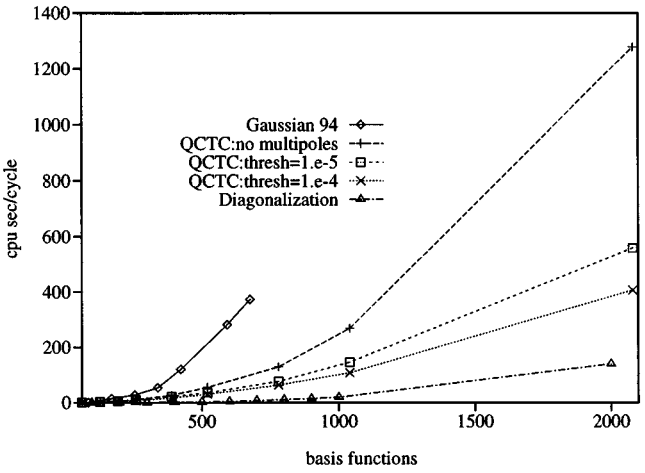

FIG. 5. Average GAUSSIAN 94 and QCTC timings for the sequence of water clusters using thresh$=10^{-5}$, thresh$=10^{-4}$, and thresh$=10^{-5}$ but no multipoles. Also shown are the diagonalization times for $N\times N$ symmetric matrices.

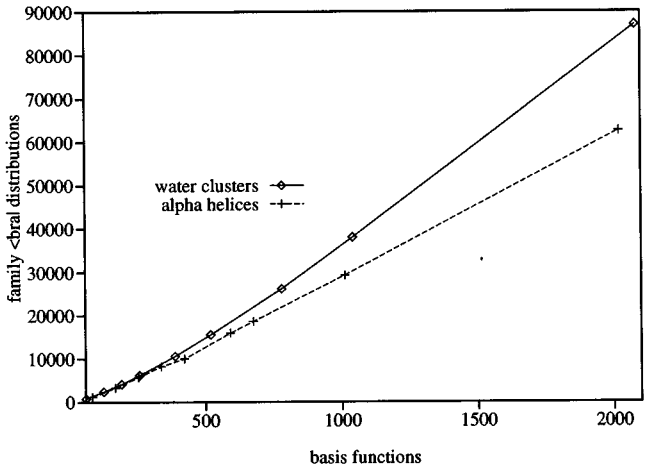

FIG. 7. The number of significant family $\langle BRA|$ distributions in the sequence of water clusters and α-helices.

inline3,aggress''). Note that even with the Direct option GAUSSIAN 94 retains as many integrals in core as possible; all GAUSSIAN 94 timings correspond to a 30 MW memory constraint. To facilitate comparison we have not used incremental Fock builds in the QCTC calculations, although doing so should result in significant acceleration. Timings corresponding to helices 10, 14 and 16, and water clusters 40 and 60, were computed as averages of the first three SCF cycles. Timings for water clusters 80 and 160, as well as for helices 24 and 48, were obtained as a single evaluation of the Coulomb matrix using a density matrix obtained from the core Hamiltonian.

In Fig. 7 the number of family $\langle BRA|$ distributions retained with thresh$=10^{-5}$ is plotted versus the number of basis functions for the sequence of water clusters and α-helices. The power dependence, obtained by fitting the last three data points in Fig. 7 to $\log(\text{number})=a+b\log(N)$, is $b=1.2$ for the water clusters and $b=1.1$ for the helices. In Table I, we list the power dependence b obtained by fitting (with least squares) the QCTC cpu times for water clusters 60, 80 and 160 and for helices 16, 24, and 48 to $\log(\text{time})=a+b\log(N)$. The scaling of GAUSSIAN 94 and QCTC without multipoles was obtained by fitting to water clusters 20, 40, and 60 and to helices 10, 14 and 16.

Errors in converged total energies obtained with SUPERMOLECULE/QCTC as well as errors in the Coulomb energy corresponding to the first SCF cycle are shown in Figs. 8 and 9, for the sequence of water clusters and helices respectively.

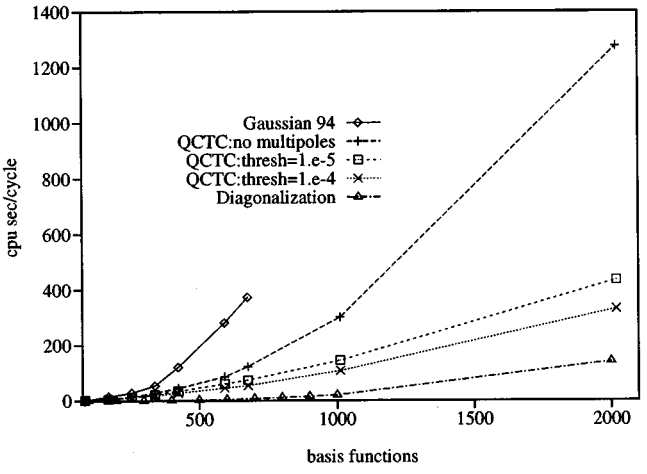

FIG. 6. Average GAUSSIAN 94 and QCTC timings for the sequence of α-helices using thresh$=10^{-5}$, thresh$=10^{-4}$, and thresh$=10^{-5}$ but no multipoles. Also shown are the diagonalization times for $N\times N$ symmetric matrices.

B. Discussion

Our current version of QCTC is competitive at the HF/3-21G level of theory and scales below N^2 for systems of chemical relevance as shown in Figs. 5–6 and summarized in Table I. As evidenced by Figs. 5 and 6, thresholding electrostatic interactions with Eq. (49), and computing their contribution to the Coulomb matrix introduces negligible overhead. This is a particular advantage of both the BH scheme, and the fast methods we employ for computing high-order Cartesian multipole expansions.[89]

TABLE I. Power dependence of GAUSSIAN 94 and QCTC.

Method	Power dependence	
	Water clusters	α-helices
GAUSSIAN 94	2.5	2.4
QCTC: no multipoles	2.3	2.1
QCTC: thresh$=10^{-5}$	2.0	1.6
QCTC: thresh$=10^{-4}$	1.9	1.6

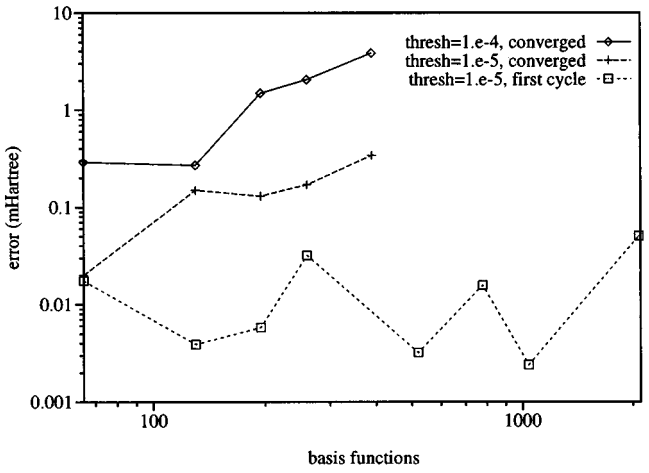

FIG. 8. Errors in the converged HF/3-21G total energies corresponding to water clusters 5, 10, 15, 20 and 30 shown in Fig. 3, and in the first SCF cycle Coulomb energies corresponding to the larger sequence of water clusters.

The errors incurred by the independent thresholding of $\langle BRA|$s and $|KET\rangle$s and by the thresholding of multipolar interactions, shown in Figs. 8 and 9, are contained by the thresholding parameter. In particular, errors in the converged SCF total energies obtained with thresh$=10^{-4}$ and thresh$=10^{-5}$ are separated by roughly an order of magnitude. Further, the reasonable behavior of first cycle Coulomb energies indicate that errors in converged total energies will continue to be well behaved for the entire sequence of structures considered here.

Even without the multipole approximation, QCTC is competitive due to the simplified HGTF representation of the density (see Sec. III) and the independent thresholding of family $\langle BRA|$s and $|KET\rangle$s (see Sec. VI). Thresholding primitive families as we have done excludes significant portions of

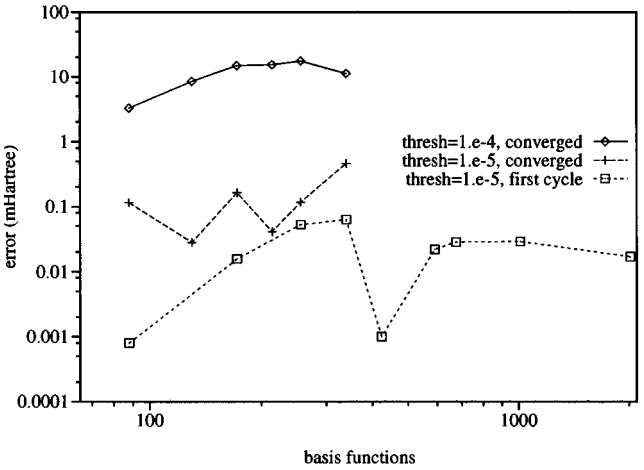

FIG. 9. Errors in the converged HF/3-21G total energies corresponding to helices 2, 4, 6 and 8 shown in Fig. 4, and in the first SCF cycle Coulomb energies corresponding to the larger sequence of helices.

work that is routinely performed by standard electronic structure programs. This is because the batch-wise calculation of a contracted quartet links the evaluation of all primitive integrals in a batch to those involving the largest radial overlaps. This effect may be clearly observed in Table I, where QCTC without the multipole approximation has approached the N^2 limit more closely than has GAUSSIAN 94. A further benefit of working with an uncontracted basis is that such calculations yield lower total energies and are generally more accurate, although that advantage has not been taken into account in the comparisons made here.

The fast timings achieved by QCTC are also due to the relatively efficient implementation of the gamma functions, $F_m(x)$, which dominate the evaluation of R_{lmn} for small ℓ. These gamma functions are computed using three-term Chebychev interpolation,[99–103] with expansion coefficients that have been computed and tabulated using MATHEMATICA[104] and the methods outlined in Ref. 103.

Although fast, the scaling of our method with the molecular sequences we have examined is not dramatically close to N. This is because the calculations are dominated by the computation of near-field interactions which scale only slightly better than N^2. Clearly, the aggressive use of the multipole approximation should result in near-field computations that scale as N.[26] However, in the current implementation we have applied the multipole approximation in the most convenient way, that is, in a way that yields the smallest execution times for small to medium sized systems. To do this we have combined distributions of all extents in each cell to reduce overhead of the multipole method, and we have used large cells to improve vectorization of the near-field integral evaluation. In doing so, we have obtained speedups of 3-4 for systems with $N \lesssim 2000$ by using the multipole approximation. Ultimately, we expect that the current implementation of QCTC will achieve an order N scaling for evaluation of near-field contributions, but we have not been able to probe this regime. For finite systems, the fastest execution times are not strictly tied to the lowest N-dependence; constants of proportionality can vary dramatically with the algorithm, its implementation and the level of precision required. This is important as fast methods stand to benefit a wide range of endeavors involving systems that are not large enough to fully access the asymptotic regime.

One alternative to the approach we have explored here is decomposition of the density into characteristic length scales, rather than clumping all extents in a given cell. This approach is similar to the modified WSI considered by White *et al.*,[28] and also has much in common with wavelet theory and multiresolution analysis.[105–107] By resolving the density into components with different rates of decay, the multipole approximation may be applied most aggressively, particularly within the Barnes-Hut approach. However, to reduce overhead the moments corresponding to different extents must also be combined as much as possible. We envision a scheme involving a 2^4-tree in which the distribution exponents are treated as an extra dimension. Evaluation of the far-field potential starts with the largest cell containing the

most distributions. As the tree is descended, multipole and penetration acceptability criteria (MAC and PAC) are used together. If for example, charge penetration is non-negligible, the next cell corresponding to the *same space* but omitting moments corresponding to the largest extents is considered. Failure to meet either MAC or PAC results in further decomposition of the density into increasing levels of spatial and functional refinement as the tree is traversed.

VIII. CONCLUSIONS

We have introduced a class of fast methods that are founded upon representation of the density in a HGTF basis, extend to the agglomeration of HGTFs at common centers by translation via Eq. (23), and culminate in the reduction of these translated HGTFs to multipole expansions in the far-field limit. Based on these developments, we have implemented a quantum chemical tree code and used it to obtain sub-N^2 scalings for computation of the Coulomb matrix. Importantly, the efficiency of our method does *not* depend critically on sacrifices in precision and, as in standard direct methods, trade-offs between speed and precision are easily controlled with a single parameter. While these results are encouraging, additional improvements are yet to be realized, both from optimization of the code and by major developments such as multiresolution and the fast Gauss transform.

The fast HGTF-based methods we have introduced here may be easily extended to the computation of other integrals including derivatives of the Coulomb matrix and integrals of the form $\int d\mathbf{r}d\mathbf{r}'\rho_{ab}(\mathbf{r})x(\mathbf{r},\mathbf{r}')\rho(\mathbf{r}')$. Because the fast HGTF-based methods retain the convenience of standard CGTF-based two-electron integrals, we foresee no difficulties integrating them into the well developed methods of molecular orbital theory. For example, within the Møller-Plesset family of perturbation methods the energy expressions can be rewritten in alternative forms that resemble the Hartree-Fock equations,[36–38] allowing the identification of Coulomb- and exchange-like contributions. Combining these techniques with the fast-HGTF based methods introduced here may make very large systems accessible not only to SCF calculations, but also to correlated methods.

We have avoided making claims about the asymptotic behavior of our method, choosing rather to present empirical results. Nevertheless, a few comments regarding the oft-cited $\mathcal{O}(N)$ or $\mathcal{O}(N\log N)$ behavior of the various hierarchical methods are in order. First of all, it is a matter of contention whether or not $\mathcal{O}(N)$ scaling can be achieved for arbitrary distributions of point charges (see Sec. II and also Ref. 63). Secondly, the hidden constants of proportionality in asymptotic estimates are important, are certain to vary between implementations and platforms, and may dramatically outweigh $\log N$ for all accessible N. Finally, in our opinion, the central issue in the adaptation of hierarchical multipole methods to quantum chemistry is not which scales more favorably for ideal systems of point charges, but which facilitates the most aggressive use of the multipole approximation and which accommodates the most efficient computation of near-field interactions.

ACKNOWLEDGMENTS

This work was supported by the Minnesota Supercomputer Institute, and by the National Science Foundation with Grant No. CHE-9223782. Matt Challacombe acknowledges a CISE postdoctoral fellowship from the NSF with matching support from MSI. Valuable discussions with Dr. R. Kutteh, Dr. A. Grama, and Dr. J. Salmon are gratefully acknowledged. Thanks are also due to Dr. J. Mertz of Cray Research Inc. for supplying the geometries of representative water clusters.

[1] C. Roothaan, Rev. Mod. Phys. **23**, 69 (1951).
[2] G. G. Hall, Proc. R. Soc. London Ser. A **205**, 541 (1951).
[3] J. A. Pople and R. K. Nesbet, J. Chem. Phys. **22**, 571 (1954).
[4] P. O. Löwdin, Phys. Rev. **97**, 1490 (1955).
[5] R. McWeeny, Rev. Mod. Phys. **126**, 1028 (1962).
[6] S. F. Boys, Proc. R. Soc. London, Ser. A **200**, 542 (1950).
[7] V. Dyczmons, Theoret. Chim. Acta **28**, 307 (1973).
[8] R. Ahlrichs, Theoret. Chim. Acta **33**, 157 (1974).
[9] G. Karlström, J. Comput. Chem. **2**, 33 (1981).
[10] J. Almlöf, K. Faegri, and K. Korsell, J. Comput. Chem. **3**, 385 (1982).
[11] D. Cremer and J. Gauss, J. Comput. Chem. **7**, 274 (1986).
[12] M. Häser and R. Ahlrichs, J. Comput. Chem. **10**, 104 (1989).
[13] S. Obara and A. Saika, J. Chem. Phys. **84**, 3963 (1985).
[14] M. Head-Gordon and J. A. Pople, J. Chem. Phys. **89**, 5777 (1988).
[15] P. M. W. Gill, M. Head-Gordon, and J. A. Pople, Int. J. Quantum Chem. Symp. **23**, 269 (1989).
[16] T. P. Hamilton and H. F. Schaefer, Chem. Phys. **150**, 163 (1991).
[17] T. P. Hamilton and H. F. Schaefer, Can. J. Chem. **70**, 416 (1992).
[18] P. M. W. Gill and J. A. Pople, Int. J. Quantum Chem. **40**, 753 (1991).
[19] I. Panas, Chem. Phys. Lett. **184**, 86 (1991).
[20] U. Ryu, Y. S. Lee, and R. Lindh, Chem. Phys. Lett. **185**, 562 (1991).
[21] R. Lindh, Theoret. Chim. Acta **85**, 423 (1993).
[22] S. Ten-no and S. Iwata, Chem. Phys. Lett. **211**, 259 (1993).
[23] B. Johnson, P. Gill, and J. Pople, Chem. Phys. Lett. **206**, 229 (1993).
[24] P. M. W. Gill, Adv. Quantum Chem. **25**, 141 (1994).
[25] D. L. Strout and G. E. Scuseria, J. Chem. Phys. **102**, 8448 (1995).
[26] I. Panas, J. Almlöf, and M. W. Feyereisen, Int. J. Quantum Chem. **40**, 797 (1991).
[27] V. Termath and N. C. Handy, Chem. Phys. Lett. **230**, 17 (1994).
[28] C. A. White, B. Johnson, P. Gill, and M. Head-Gordon, Chem. Phys. Lett. **230**, (1994).
[29] H. Böhm and R. Ahlrichs, J. Chem. Phys. **115**, 2028 (1982).
[30] F. Maeder, J. Chem. Phys. **88**, 4934 (1988).
[31] E. Hernández, M. J. Gillan, and C. M. Goringe, e-print, 1995, available at http://www.chem.brown.edu/chem-ph.html.
[32] R. G. Parr and W. Yang, *Density-functional Theory of Atoms and Molecules* (Oxford University, Oxford, 1989).
[33] E. S. Kryachko and E. V. Ludeña, *Energy Density Functional Theory of Many Electron Systems* (Kluwer Academic, Boston, 1990).
[34] B. Johnson, P. Gill, and J. Pople, J. Chem. Phys. **98**, 5612 (1993).
[35] A. D. Becke, J. Chem. Phys. **98**, 5648 (1993).
[36] J. Almlöf, Chem. Phys. Lett. **181**, 319 (1991).
[37] M. Häser and J. Almlöf, J. Chem. Phys. **96**, 489 (1992).
[38] M. Häser, Theoret. Chim. Acta **87**, 147 (1993).
[39] A. L. Sargent, J. Almlöf, and M. W. Feyereisen, SIAM News **26**, 14 (1993).
[40] J. Barnes and P. Hut, Nature (London) **324**, 446 (1986).
[41] L. Hernquist, Ap. J. Suppl. **64**, 715 (1987).
[42] J. E. Barnes and P. Hut, Ap. J. Suppl. **70**, 389 (1989).
[43] M. S. Warren and J. K. Salmon, in *Proceedings SUPERCOMPUTING '93* (IEEE Computer Society, Los Alamitos, 1993), pp. 12–21.
[44] S. Pfalzner and P. Gibbon, Comput. Phys. Commun. **79**, 24 (1994).
[45] J. K. Salmon, M. S. Warren, and G. S. Winckelmans, Int. J. Super. Appl. **8**, 129 (1994).
[46] M. S. Warren and J. K. Salmon, Comput. Phys. Commun. **87**, 266 (1995).
[47] L. Greengard and V. Rokhlin, J. Comput. Phys. **73**, 325 (1987).
[48] K. E. Schmidt and M. A. Lee, J. Stat. Phys. **63**, 1223 (1991).

[49] H. Petersen, D. Soelvason, J. W. Perram, and E. R. Smith, J. Chem. Phys. **101**, 8870 (1994).
[50] H. Petersen, E. R. Smith, and D. Soelvason, Proc. R. Soc. London, Ser. A **448**, 401 (1994).
[51] C. A. White and M. Head-Gordon, J. Chem. Phys. **101**, 6593 (1994).
[52] W. D. Elliot and J. A. Board, Jr., Technical Report No. 94-001, Duke University Dept. of Electrical Engineering, (unpublished), available at http://www.ee.duke.edu/Research/SciComp/papers.html.
[53] J. A. Board, Jr., Z. S. Hakura, W. D. Elliot, and W. T. Rankin, Technical Report No. 94-006, Duke University Dept. of Electrical Engineering, (unpublished), available at http://www.ee.duke.edu/Research/SciComp/papers.html.
[54] R. Kutteh, E. Aprà, and J. Nichols, Chem. Phys. Lett. **238**, 173 (1995).
[55] J. A. Board *et al.*, Chem. Phys. Lett. **198**, 89 (1992).
[56] H. Q. Ding, N. Karasawa, and W. A. Goddard III, J. Chem. Phys. **97**, 4309 (1992).
[57] H. Ding, N. Karasawa, and W. A. Goddard III, Chem. Phys. Lett. **196**, 6 (1992).
[58] R. Kutteh and J. B. Nicholas, Comput. Phys. Commun. **86**, 227 (1995).
[59] R. Kutteh and J. B. Nicholas, Comput. Phys. Commun. **86**, 236 (1995).
[60] A. Y. Grama, V. Kumar, and A. Sameh, in *Proceedings SUPERCOMPUTING '94* (IEEE Computer Society, Los Alamitos, 1994), pp. 439–448.
[61] G. Blellock and G. Narlikar, e-print, 1995, available at http://www.cs.cmu.edu/afs/cs.cmu.edu/user/guyb/www/publications.html.
[62] L. Greengard and V. Rokhlin, Comput. Phys. **4**, 142 (1990).
[63] S. Aluru, G. M. Prabhu, and J. Gustafson, in *Proceedings SUPERCOMPUTING '94* (IEEE Computer Society, Los Alamitos, 1994), pp. 420–428.
[64] L. S. Nyland, J. F. Prins, and J. H. Reif, in *DAGS/PC Workshop on Practical Parallel Algorithms* (Dartmouth University, Hanover, NH, 1993).
[65] A. Windemuth, in *Parallel Computing in Computational Chemistry* (ACS, Washington, DC, 1995).
[66] P. B. Callahan and S. R. Kosaraju, J. ACM **42**, 67 (1995).
[67] M. C. Strain and G. E. Scuseria, Science **271**, 51 (1996).
[68] L. McMurchie, Ph.D. thesis, University of Seattle, 1977.
[69] L. E. McMurchie and E. R. Davidson, J. Comput. Phys. **26**, 218 (1978).
[70] V. R. Saunders, in *Methods in Compuational Molecular Physics*, edited by G. H. F. Diercksen and S. Wilson (Reidel, Boston, 1983), pp. 1–36.
[71] I. Shavitt, Meth. Comput. Phys. **2**, 1 (1963).
[72] P. J. Davis, in *Handbook of Mathematical Functions*, 9th ed., edited by M. Abramowitz and I. A. Stegun (Dover, New York, 1987), pp. 260–2.
[73] G. R. Ahmadi and J. Almlöf, Chem. Phys. Lett. **246**, 364 (1996).
[74] C. A. White and M. Head-Gordon, J. Chem. Phys. **104**, 2620 (1996).
[75] W. J. Hehre, L. Radom, P. von Schleyer, and J. A. Pople, *Ab initio Molecular Orbital Theory* (Wiley, New York, 1986).
[76] S. Huzinaga, Comput. Phys. Rep. **2**, 279 (1985).
[77] S. Huzinaga, M. Klobukowski, and H. Tatewaki, Can. J. Chem. **63**, 1812 (1985).
[78] S. Huzinaga and B. Miguel, Chem. Phys. Lett. **175**, 289 (1990).
[79] S. Huzinaga and M. Klobukowski, Chem. Phys. Lett. **212**, 260 (1993).
[80] R. Bardo and K. Ruedenberg, J. Chem. Phys. **60**, 918 (1974).
[81] E. Clementi and G. Corongiou, Chem. Phys. Lett. **90**, 359 (1982).
[82] S. Wilson, Theoret. Chim. Acta **57**, 53 (1980).
[83] S. Wilson, Theoret. Chim. Acta **58**, 31 (1980).
[84] L. Greengard and J. Strain, J. Sci. Stat. Comput. **12**, 79 (1991).
[85] J. Strain, J. Sci. Stat. Comput. **12**, 1131 (1991).
[86] J. Strain, J. Sci. Comput. **15**, 185 (1994).
[87] E. Hille, Ann. Math. **27**, 427 (1926).
[88] C. Cohen-Tannoudji, B. Diu, and F. Laloë, *Quantum Mechanics* (Wiley New York, 1977), Vol. II, see Appendix II for a useful discussion of the Dirac delta function and its derivatives.
[89] M. Challacombe, E. Schwegler, and J. Almlöf, Chem. Phys. Lett. **241**, 67 (1995), a number of typographical errors were introduced into this letter. A clean version is available from the first author.
[90] W. H. Press, in *The Use of Supercomputers in Stellar Dynamics* (Springer, New York, 1986), pp. 439–448.
[91] P. M. W. Gill, B. G. Johnson, and J. A. Pople, Chem. Phys. Lett. **217**, 65 (1994).
[92] S. R. Gadre and R. K. Pathak, Adv. Quantum Chem. **22**, 211 (1991).
[93] J. L. Whitten, J. Chem. Phys. **58**, 4496 (1973).
[94] J. D. Power and R. M. Pitzer, Chem. Phys. Lett. **24**, 478 (1974).
[95] J. Almlöf and M. Feyereisen, SUPERMOLECULE, a program for *ab initio* electronic structure calculations.
[96] V. R. Saunders, C. Freyria-Fava, L. S. R. Dovesi, and C. Roetti, Mol. Phys. **77**, 629 (1992).
[97] M. J. Frisch *et al.*, GAUSSIAN 94, *Revision B.3* (GAUSSIAN, Inc., Pittsburgh, 1994).
[98] *NAG Fortran Library Manual, Mark 15* (Numerical Algorithms Group Limited, 1991).
[99] L. L. Shipman and R. E. Christoffersen, Comput. Phys. Comm. **2**, 201 (1971).
[100] S. T. Elbert and E. R. Davidson, J. Comput. Phys. **16**, 391 (1974).
[101] P. Gill, B. Johnson, and J. Pople, Int. J. Quantum Chem. **40**, 745 (1991).
[102] S. Yahiro and Y. Gondo, J. Comput. Chem. **13**, 12 (1992).
[103] M. Challacombe, Ph.D. thesis, Florida State University, 1994.
[104] S. Wolfram, *Mathematica, A System for Doing Mathematics by Computer*, 2nd ed. (Addison-Wesley, Redwood City, 1991).
[105] I. Daubechies, *Ten Lectures on Wavelets* (SIAM, Philidelphia, 1992).
[106] C. K. Chui, *Wavelets - A Tutorial in Theory and Applications* (Academic, New York, 1992).
[107] M. Gross, R. Gatti, and O. Staadt, Technical Report No. TR-230, Computer Science Department, ETH Z üric, (unpublished), available at http://www.inf.ethz.ch/department/IS/cg/html/papers.html.
[108] *InsightII User Guide* (Biosym Technologies, 1992).